

NOMENCLATURE

LATIN SYMBOLS

a	leaf area density	$\text{m}^2 \text{m}^{-3}$
A	area	m^2
A_f	frontal area	m^2
A_L	net leaf area	m^2
A_n	assimilation rate	$\text{mol m}^{-2} \text{s}^{-1}$
b	Vogel exponent	-
c_d	leaf drag coefficient	-
C_d	drag coefficient	-
c_p	specific heat (at constant pressure)	$\text{J kg}^{-1} \text{K}^{-1}$
c_a^*	reference CO_2 concentration	mol mol^{-1}
C	aerodynamic resistance coefficient	$\text{s}^{0.5} \text{m}^{-1}$
$C_{o,a}$	oxygen concentration	mol mol^{-1}
D	diameter	m
D	vapor pressure deficit	kPa
D	vapor pressure deficit	$\text{Pa Pa}^{-1}, \text{mol mol}^{-1}$
e_m	maximum quantum efficiency of the leaf	-
E	leaf transpiration flux	kg s^{-1}
f_c	CO_2 assimilation (photosynthesis) rate	$\text{mol m}^{-2} \text{s}^{-1}$
f_v	transpiration rate	$\text{mol m}^{-2} \text{s}^{-1}$
F	force	N
F_d	drag force	N
g	gravitational acceleration	$\text{m}^2 \text{s}^{-1}$
g_l	liquid water flux	$\text{kg m}^{-2} \text{s}^{-1}$
g_v	water vapor flux	$\text{kg m}^{-2} \text{s}^{-1}$
$g_{v,leaf}$	water vapor mass flux	$\text{kg m}^{-2} \text{s}^{-1}$
$g_{v,root}$	root water uptake	$\text{kg m}^{-2} \text{s}^{-1}$
$G_{v,root}$	net root water uptake	kg s^{-1}
$G_{v,xylem}$	net xylem water flux	kg s^{-1}
h	enthalpy	J kg^{-1}
$h_{c,h}$	convective heat transfer coefficient	$\text{W m}^{-2} \text{K}^{-1}$

$h_{c,m}$	convective mass transfer coefficient	m s^{-1}
H	height	m
HU	Hounsfield units	-
I	turbulence intensity	%
k	turbulent kinetic energy	$\text{m}^2 \text{s}^{-2}$
k_{st}	stomatal conductance	$\text{mol m}^{-2} \text{s}^{-1}$
k_{st}^*	effective stomatal conductance	$\text{mol m}^{-2} \text{s}^{-1}$
K	permeability	m^2
K	hydraulic conductivity	m s^{-1}
K_{lp}	liquid water permeability	s
K_{vp}	water vapor permeability	s
K_{vT}	water vapor permeability due to temperature	s
K_c	Michaelis constant for CO_2	???
K_o	Michaelis constant for O_2	???
l	length	m
l	characteristic leaf size	m
\mathcal{L}	Lagrangian	-
L_v	latent heat of vaporization for water ($= 2.5 \times 10^6$)	J kg^{-1}
m	mass	kg
M	molar mass	kg mol^{-1}
M_a	molar mass of dry air ($= 0.028\,966$)	kg mol^{-1}
M_v	molar mass of water vapor ($= 0.018\,015\,34$)	kg mol^{-1}
n	Van Genuchten parameter	-
p_c	capillary pressure	Pa
p_l	liquid pressure	Pa
p_l	gas phase pressure	Pa
p_v	partial vapor pressure	Pa
$p_{v,i}$	intercellular vapor pressure	Pa
$p_{v,sat}$	saturation vapor pressure	Pa
P	pressure	Pa
Pr	Prandtl number	-
Pr_t	turbulent Prandtl number	-
q	heat flux	W m^{-2}
$q_{lat,lat}$	latent heat flux from leaf	W m^{-2}
q_r	net radiative heat flux	W m^{-2}
$q_{r,sw}$	short-wave radiative heat flux	W m^{-2}
$q_{r,lw}$	long-wave radiative heat flux	W m^{-2}

$q_{rad,lat}$	radiative heat flux into leaf	$W m^{-2}$
$q_{sen,lat}$	sensible heat flux from leaf	$W m^{-2}$
Q_p	flux of incoming PAR	???
r	root area density	$m^2 m^{-3}$
r_a	aerodynamic resistance	$s m^{-1}$
r_s	stomatal resistance	$s m^{-1}$
R	universal gas constant (= 8.314 459 8)	$J mol^{-1} K^{-1}$
RAI	root area index	$m^2 m^{-2}$
Re	Reynolds number	-
R_v	specific gas constant of dry air (= 287.042)	$J kg^{-1} K^{-1}$
R_v	specific gas constant of water vapor (= 461.524)	$J kg^{-1} K^{-1}$
Sc_t	turbulent Schmidt number	-
s_ϵ	volumetric TDR source	$W m^{-3} s^{-1}$
s_ρ	volumetric mass source	$kg m^{-3} s^{-1}$
s_k	volumetric TKE source	$W m^{-3}$
$s_{q,r}$	volumetric radiative source	$W m^{-3}$
s_r	volumetric root water uptake source	$kg m^{-3} s^{-1}$
s_T	volumetric temperature source	$K m^{-3}$
s_u	volumetric momentum source	$N m^{-3}$
s_w	volumetric humidity source	$kg kg^{-1} s^{-1}$
S_l	liquid saturation	-
t	time	s
T	temperature	K
T_g	ground temperature	K
T_L	leaf temperature	K
T_{sky}	sky temperature	K
TR	net hourly transpiration rate	$g h^{-1}$
u	velocity	$m s^{-1}$
u_*	friction velocity	$m s^{-1}$
U	mean wind speed	$m s^{-1}$
U_{ref}	reference velocity	$m s^{-1}$
$UTCI$	universal thermal climate index	$^{\circ}C$
V_{cmax}	maximum carboxylation capacity	???
w	moisture content	$kg m^{-3}$
w_a	dry air content	$kg m^{-3}$
w_{cap}	capillary moisture content	$kg m^{-3}$
w_l	liquid water content	$kg m^{-3}$

w_s	solid matrix water content	kg m^{-3}
w_v	water vapor content	kg m^{-3}
z	vertical height	m
z_0	aerodynamic roughness height	m

GREEK SYMBOLS

α	aerodynamic porosity	-
α^{2D}	2D aerodynamic porosity	-
α_p	leaf absorptivity of PAR	-
β	optical porosity	-
β	volumetric thermal expansion coefficient	K^{-1}
β_p	fraction of MKE converted to TKE	-
β_d	fraction of TKE shortcut to TDR	-
γ	apparent quantum yield	-
δ_v	water vapor diffusion coefficient	s
ε	turbulent kinetic energy dissipation rate	$\text{m}^2 \text{s}^{-3}$
κ	von Kármán constant (= 0.41)	-
λ	thermal conductivity	$\text{W m}^{-1} \text{K}^{-1}$
λ	Lagrange multiplier	mol mol^{-1}
μ	attenuation coefficient	m^{-1}
μ	chemical potential	J mol^{-1}
μ	dynamic viscosity	$\text{kg m}^{-1} \text{s}^{-1}$
ν	kinematic viscosity	$\text{m}^2 \text{s}^{-1}$
ν_t	turbulent viscosity	$\text{m}^2 \text{s}^{-1}$
ρ	density	kg m^{-3}
ρ_a	density of air	kg m^{-3}
ρ_l	density of liquid water (= 1000)	kg m^{-3}
ρ_s	density of solid matrix	kg m^{-3}
σ_v	Schmidt number	-
σ_{v_t}	turbulent Schmidt number	-
ϕ_0	open porosity	$\text{m}^3 \text{m}^{-3}$
ψ	shelter parameter	-
ψ_g	gravitational potential	Pa
ψ_L	leaf water potential	Pa
ψ_R	root water potential	Pa

ψ_s	soil water potential	Pa
Ω	domain	-
Ω_a	air domain	-
Ω_s	soil domain	-

SUBSCRIPTS

<i>eff</i>	effective
<i>g</i>	gas
<i>g</i>	ground
<i>i</i>	intercellular
<i>l</i>	liquid (water)
<i>lw</i>	long-wave
<i>L</i>	leaf
<i>o</i>	open
<i>pore</i>	pore
<i>ref</i>	reference
<i>root</i>	root
<i>sat</i>	saturated
<i>R</i>	root
<i>s</i>	solid
<i>s</i>	soil
<i>sky</i>	sky
<i>sw</i>	short-wave
<i>t</i>	time
<i>v</i>	vapor
<i>xylem</i>	xylem

ACRONYMS

ABL	atmospheric boundary layer
CFD	computational fluid dynamics
CHTC	convective heat transfer coefficient
CMTC	convective mass transfer coefficient

CT	computational tomography
DEHS	Di-Ethyl-Hexyl-Sebacat
DIG	diagonal-based incomplete Cholesky
DNS	direct numerical simulation
ETHZ	Eidgenössische Technische Hochschule Zürich
FOV	field of view
FFT	fast Fourier transformation
FVM	finite volume method
HPC	high performance computing
LAI	leaf area index
LAI	leaf area density
LDPE	low-density Polyethylene
LES	large eddy simulation
LHS	left hand side
MOE	modulus of elasticity
PAR	photosynthetically active radiation
PCG	preconditioned conjugate gradient
PIV	particle image velocimetry
PPM	parts per million
RAI	root area index
REV	representative elementary volume
RANS	Reynolds-averaged Navier-Stokes
RHS	right hand side
ROI	region of interest
SPIV	stereoscopic particle image velocimetry
TDR	turbulent dissipation rate
TKE	turbulent kinetic energy
UHI	urban heat island

UTCI	universal thermal climate index
WUE	water use efficiency

CONTENTS

Nomenclature	i
1 Numerical model for vegetation in urban areas	1
1.1 Introduction	1
1.2 Governing equations of coupled heat and moisture transport	1
1.2.1 Composition of the porous material	1
1.2.2 Water potential	2
1.2.3 Coupled transport of heat and mass	3
1.2.4 Linearized heat and mass transport equation	6
1.3 Soil-Plant-Atmosphere Continuum model	8
1.3.1 Water transport in soil-root system	9
1.3.2 Water transport in xylem	10
1.3.3 Water transport from leaf to air	11
1.3.4 Stomatal model with water stress sensitivity	13
1.3.5 Assimilation rate	16
1.3.6 Numerical strategy for solving leaf water potential	18
1.4 Coupled air-soil-vegetation-radiation model	18
1.5 Coupling algorithm	18
1.5.1 Air domain	19
1.5.2 Soil domain	19
Bibliography	21

NUMERICAL MODEL FOR VEGETATION IN URBAN AREAS

1.1 INTRODUCTION

The simplified vegetation model is described in ?? introduction the governing equation for moist flow vegetation. The vegetation model provides the necessary source/sink terms for heat, mass and momentum exchanges between vegetation and air as described in ?. Furthermore, radiation transfer within vegetation is also described in ?. For reader, a detailed derivation of the thermodynamic of the moist air is given in ?? and a detailed derivation of the governing equation of moist flow is given in ?.

In this chapter, the numerical method for modeling vegetation inside an urban area is described. The chapter focuses on coupling of the vegetation model with the of heat (incl. radiation) and mass fluxes of the urban surfaces. The governing equation for the the coupled heat and moisture transport in the porous material is first described.

1.2 GOVERNING EQUATIONS OF COUPLED HEAT AND MOISTURE TRANSPORT

1.2.1 *Composition of the porous material*

The building materials and the soil is considered as a porous material consisting of three phases: solid phase (denoted with s), liquid phase referring to liquid water (l) and the air phase which is split into dry air (a) and water vapor v (Janssen 2002; Carmeliet 2005; Defraeye 2011; Saneinejad 2013). The open porosity ϕ_o ($\text{m}^3 \text{m}^{-3}$) of the porous material is defined as:

$$\phi_o = \frac{V_{pore}}{V} \quad (1.1)$$

where V_{pore} (m^3) is the volume of open pores and V (m^3) is the total volume of the porous material S . The solid material content w_s (kg m^{-3}) is defined as:

$$w_s = (1 - \phi_o) \rho_s \quad (1.2)$$

where ρ_s (kg m^{-3}) is the solid material matrix density. Similarly the dry air w_a , water vapor w_v , liquid water w_l contents are defined as:

$$w_l = \phi_o S_l \rho_l \quad (1.3)$$

$$w_a = \phi_o (1 - S_l) \rho_a \quad (1.4)$$

$$w_v = \phi_o (1 - S_l) \rho_v \quad (1.5)$$

where they are related to the degree of liquid saturation S_l of the porous open pores:

$$S_l = \frac{\phi_{o,l}}{\phi_o} \quad (1.6)$$

with $\phi_{o,l}$ being the amount of liquid water occupied inside the open pores and ρ_a, ρ_l being the air and liquid water densities, respectively. The total moisture content w (kg m^{-3}) inside the porous material is simply the sum of liquid water and water vapor:

$$w = w_l + w_v \quad (1.7)$$

1.2.2 Water potential

Water potential is a universal parameter to determine the *water status* in any medium (Nobel 2009). In the thesis, we use it to define the water status of multiple domains such as solid porous materials (soil and building facades), plant xylem, and air. The water potential ψ (Pa) describes the chemical potential of water μ (J mol^{-1}) with respect to chemical potential of pure water $\mu^{o,l}$ (J mol^{-1}) at the same temperature, standard atmosphere and at zero level:

$$\psi = \frac{\mu - \mu^{o,l}}{V_l^o} \quad (1.8)$$

where $V_l^o = 18.0510^{-3} \text{ m}^3 \text{ mol}^{-1}$ is the molar volume of pure water in liquid phase. The water potential for pure water at standard atmosphere is $\psi = 0$ Pa. The water tends to move towards a region where $\mu - \mu^{o,w}$ is lower, i.e. in the direction of $-\nabla\psi$. The water potential is related to pressure potential, osmotic potential, matrix potential, and gravitational potential. In our study, we assume that the pressure potential gradient is negligible in the solid and we ignore the influence of osmotic potential ψ_o (Pa) as we assume we have a non-saline porous material. Therefore, only the matrix potential and gravitation potential influences the water transport:

$$\psi = \underbrace{p_c}_{\psi_c} + \underbrace{\rho_l g z}_{\psi_g} \quad (1.9)$$

where $\psi_c = p_c$ (Pa) is the capillary potential due to capillary pressure, which represents the contribution of the matrix potential, and $\psi_g = \rho_l g h$ (Pa) is the gravitational potential with $g = |g|$ (m s^{-2}) where g is the gravitational acceleration. The capillary

pressure p_c is defined as the difference between liquid and gas phase pressure, p_l and p_g , respectively:

$$p_c = p_l - p_g \quad (1.10)$$

and is related to relative humidity ϕ by the Kelvin's law:

$$p_c = \rho_l R_v T \ln(\phi) \quad (1.11)$$

The gravitational potential ψ_g (Pa) is defined as:

$$\psi_g = -\rho g \cdot x = \rho g z \quad (1.12)$$

where $g = |g|$ with z oriented upward. Thus, by taking the capillary and gravitational water potentials into account, the transport of water can be described in building materials and, more importantly, soil where the plant roots are present.

1.2.3 Coupled transport of heat and mass

Conservation of mass

The conservation of mass in the solid domain is defined as:

$$\frac{\partial w_s}{\partial t} = 0 \quad (1.13)$$

$$\frac{\partial w_a}{\partial t} + \nabla \cdot (w_a \mathbf{u}_a) = 0 \quad (1.14)$$

$$\frac{\partial w_l + w_v}{\partial t} + \nabla \cdot (w_l \mathbf{u}_l + w_v \mathbf{u}_v) = 0 \quad (1.15)$$

assuming that solid matrix does not move, mass of different phases only change due to evaporation or condensation. Other phenomena such as melting, freezing, sublimation and deposition are neglected. Assuming dry air does not contribute to moisture storage, i.e., $\partial w_a / \partial t = 0$, the conservation of mass simplifies to rate of change of moisture content $w = w_l + w_v$, from Eq. (1.15):

$$\frac{\partial w}{\partial t} = -\nabla \cdot (\mathbf{g}_l + \mathbf{g}_v) \quad (1.16)$$

where $\mathbf{g}_l \equiv w_l \mathbf{u}_l$ ($\text{kg m}^{-2} \text{s}^{-1}$) and $\mathbf{g}_v \equiv w_v \mathbf{u}_v$ ($\text{kg m}^{-2} \text{s}^{-1}$) are defined as the liquid water and water vapor fluxes, respectively. Additionally, the contribution of root water uptake due to plant transpiration is introduced through the source term s_r ($\text{kg m}^{-3} \text{s}^{-1}$):

$$\frac{\partial w}{\partial t} = -\nabla \cdot (\mathbf{g}_l + \mathbf{g}_v) + s_r \quad (1.17)$$

The sink term due to root water uptake is explained in detail later in Section 1.3. In this thesis, the conservation of mass is solved using the p_c -form Richards equation, where Eq. (1.17) becomes:

$$\frac{\partial w}{\partial p_c} \frac{\partial p_c}{\partial t} = -\nabla \cdot (\mathbf{g}_l + \mathbf{g}_v) + s_r \quad (1.18)$$

with $C_{mm} \equiv \partial w / \partial p_c$ ($\text{kg m}^{-3} \text{Pa}^{-1}$) is defined as the moisture capacity. Thus, the change in water content in the porous material is simply due to the liquid and vapor fluxes, and root water uptake. The liquid water flux \mathbf{g}_l in porous media is given by:

$$\mathbf{g}_l = -K_{lp} \nabla (p_c + \rho_l g z) \quad (1.19)$$

and assumes the air pressure effects be negligible with respect to capillary and gravitational effects, where K_{lp} (s) the liquid water permeability. We assume that the liquid water permeability is only due to pressure gradient, and the influence of thermal gradient is neglected (Carmeliet 2005). The water vapor flux in the porous media is given by:

$$\mathbf{g}_v = K_{vp} \nabla p_c + K_{vT} \nabla T \quad (1.20)$$

where

$$K_{vp} = -\delta_v \frac{p_v}{\rho_l R_v T} \quad (1.21)$$

is the water vapor permeability (s) due to pressure,

$$K_{vT} = -\delta_v \frac{p_v}{\rho_l R_v T^2} (\rho_l L_v - p_c) \quad (1.22)$$

is the water vapor permeability (s) due to temperature, and

$$\delta_v = \frac{D_{va,mat}}{R_v T} \quad (1.23)$$

is the water vapor diffusion coefficient (s) where $D_{va,mat}$ ($\text{m}^2 \text{s}^{-1}$) is the binary apparent diffusion coefficient between dry air and water vapor (Carmeliet 2005; Defraeye 2011; Saneinejad 2013; Kubilay 2014). Thus, substituting the fluxes Eqs. (1.19) and (1.20) into Eq. (1.18), the expanded form of conservation of mass is given as:

$$C_{mm} \frac{\partial p_c}{\partial t} = \nabla \cdot \left(K_{lp} \nabla (p_c + \rho_l g z) + K_{vp} \nabla p_c + K_{vT} \nabla T \right) + s_r \quad (1.24)$$

Conservation of energy

The conservation of energy is given as:

$$\frac{\partial h}{\partial t} + \nabla \cdot (h \mathbf{u}) = -\nabla \cdot \mathbf{q} \quad (1.25)$$

where h (J kg^{-1}) is the enthalpy of total solid domain:

$$h = \sum_i w_i h_i = w_s h_s + w_a h_a + w_l h_l + w_v h_v \quad (1.26)$$

and heat conduction \mathbf{q} (W m^{-2}) is given by Fourier's law as:

$$\mathbf{q} = -\lambda \nabla T \quad (1.27)$$

where T (K) is temperature, λ ($\text{W m}^{-1} \text{K}^{-1}$) is thermal conductivity.

Substituting Eq. (1.26) into Eq. (1.25) expands to:

$$\frac{\partial}{\partial t} (w_s h_s + w_a h_a + w_l h_l + w_v h_v) + \nabla \cdot (w_a \mathbf{g}_a + w_l \mathbf{g}_l + w_v \mathbf{g}_v) = -\nabla \cdot \mathbf{q} \quad (1.28)$$

and assuming dry air and water vapor does not contribute to heat storage, i.e., $\partial w_a h_a / \partial t \approx 0$ and $\partial w_v h_v / \partial t \approx 0$, and convection term of dry air is negligible $\nabla \cdot w_a \mathbf{g}_a \approx 0$, Eq. (1.28) simplified to:

$$\frac{\partial (w_s h_s + w_l h_l)}{\partial t} + \nabla \cdot (w_l \mathbf{g}_l + w_v \mathbf{g}_v) = -\nabla \cdot \mathbf{q} \quad (1.29)$$

The enthalpies of solid h_s , liquid water h_l and water vapor h_v are defined as:

$$h_s = c_{ps} (T - T_{ref}) \quad (1.30)$$

$$h_l = c_{pl} (T - T_{ref}) \quad (1.31)$$

$$h_v = c_{pv} (T - T_{ref}) + L_v \quad (1.32)$$

and L_v is the latent heat of vaporization of water. Substituting Eqs. (1.30) to (1.32) into Eq. (1.29), the conservation of energy is given as:

$$\begin{aligned} & \left(c_{ps} w_s + c_{pl} w \right) \frac{\partial T}{\partial t} + \left[c_{pl} (T - T_{ref}) \frac{\partial w}{\partial p_c} \right] \frac{\partial p_c}{\partial t} = \\ & -\nabla \cdot \left\{ \mathbf{q} + \underbrace{c_{pl} (T - T_{ref}) \mathbf{g}_l}_{q_l} + \underbrace{\left[c_{pv} (T - T_{ref}) + L_v \right] \mathbf{g}_v}_{q_v} \right\} \end{aligned} \quad (1.33)$$

where:

$$C_{TT} = c_{ps} w_s + c_{pl} w \quad (1.34)$$

$$C_{Tp} = c_{pl} (T - T_{ref}) \frac{\partial w}{\partial p_c} \quad (1.35)$$

are the thermal capacity terms. Substituting liquid and vapour fluxes, Eqs. (1.19) and (1.20), respectively, thermal capacities Eqs. (1.34) and (1.35) and heat conduction Eq. (1.27) into conservation of energy expands Eq. (1.33) to:

$$\begin{aligned}
 C_{TT} \frac{\partial T}{\partial t} + C_{Tp} \frac{\partial p_c}{\partial t} = \nabla \cdot \bigg(& \lambda \nabla T + K_{lp} c_{pl} (T - T_{ref}) \nabla p_c \\
 & + K_{lp} c_{pl} (T - T_{ref}) \rho_l g z \\
 & - K_{vp} [c_{pv} (T - T_{ref}) + L_v] \nabla p_c \\
 & - K_{vT} [c_{pv} (T - T_{ref}) + L_v] \nabla T \bigg)
 \end{aligned} \tag{1.36}$$

1.2.4 Linearized heat and mass transport equation

In the present study, the conservation of mass and energy is coupled together as a heat and mass model (HAM) according to (Janssen 2002; Carmeliet 2005; Defraeye 2011; Saneinejad 2013; Kubilay et al. 2018). Due to the shape of the water retention curve and the hydraulic conductivity curve, as shown in Fig. 1.1, the Richards equation is highly non-linear. Therefore, the numerical solution of the equation is very sensitive to convergence tolerance and requires linearization techniques to maintain accuracy and computational efficiency. So, methods such as fixed-point Picard iterations is used to solve the non-linear equations. More details on the discretization is provided in Janssen (2002), Liu (2012), and Kubilay et al. (2018).

The conservation of mass (i.e., the moisture transport equation), Eq. (1.24), in the linearized form is given as:

$$\begin{aligned}
 C_{mm}^{n+1,k} \frac{p_c^{n+1,k+1} - p_c^n}{\Delta t} = \nabla \cdot \bigg(& K_{lp}^{n+1,k} \nabla (p_c^{n+1,k+1} + \rho_l g z) \\
 & + K_{vp}^{n+1,k} \nabla p_c^{n+1,k+1} \\
 & + K_{vT}^{n+1,k} \nabla T^{n+1,k} \bigg) \\
 & + s_r^{n+1,k+1}
 \end{aligned} \tag{1.37}$$

where the capacity, permeabilities and temperature are determined from the previous Picard iteration (k). The subscript (n) denotes the global (i.e., outer) time step of t and k denoting the internal Picard iteration step. When the Picard solution approaches convergence, i.e., $p_c^{n+1,k} \rightarrow p_c^{n+1,k+1}$, $\partial w / \partial p_c$ becomes negligible resulting in larger mass

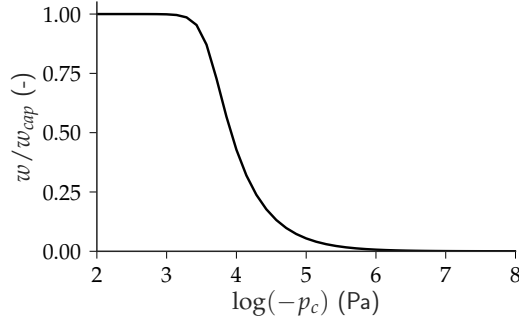


Figure 1.1: Typical non-linear moisture water retention curve for a material which is capillary saturated.

conservation errors. The error is minimized by formulating the Richard's equation in mixed-form (Liu 2012):

$$\begin{aligned}
 C_{mm}^{n+1,k} \frac{p_c^{n+1,k+1} - p_c^n}{\Delta t} = \nabla \cdot \left(K_{lp}^{n+1,k} \nabla \left(p_c^{n+1,k+1} + \rho_l g z \right) \right. \\
 \left. + K_{vp}^{n+1,k} \nabla p_c^{n+1,k+1} \right. \\
 \left. + K_{vT}^{n+1,k} \nabla T^{n+1,k} \right) \\
 + s_r^{n+1,k+1} - \frac{w^{n+1,k+1} - w^n}{\Delta t}
 \end{aligned} \tag{1.38}$$

where an additional moisture change term is added.

The linearized form of the heat equation is given as:

$$\begin{aligned}
 C_{TT}^{n+1,k} \frac{T^{n+1,k+1} - T^n}{\Delta t} = \nabla \cdot \left(\lambda \nabla T^{n+1,k+1} \right. \\
 + K_{lp}^{n+1,k} c_{pl} \left(T^{n+1,k+1} - T_{ref} \right) \nabla p_c^{n+1,k+1} \\
 + K_{lp}^{n+1,k} c_{pl} \left(T^{n+1,k+1} - T_{ref} \right) \rho_l g z \\
 - K_{vp}^{n+1,k} \left[c_{pv} \left(T^{n+1,k+1} - T_{ref} \right) + L_v \right] \nabla p_c^{n+1,k} \\
 \left. - K_{vT}^{n+1,k} \left[c_{pv} \left(T^{n+1,k+1} - T_{ref} \right) + L_v \right] \nabla T^{n+1,k+1} \right)
 \end{aligned} \tag{1.39}$$

where the capillary pressure time derivative term is ignored. The mixed-form the heat equation is given as:

$$\begin{aligned}
C_{TT}^{n+1,k} \frac{T^{n+1,k+1} - T^n}{\Delta t} = & \nabla \cdot \left(\lambda \nabla T^{n+1,k+1} \right. \\
& + K_{lp}^{n+1,k} c_{pl} \left(T^{n+1,k+1} - T_{ref} \right) \nabla p_c^{n+1,k+1} \\
& + K_{lp}^{n+1,k} c_{pl} \left(T^{n+1,k+1} - T_{ref} \right) \rho_l g z \\
& - K_{vp}^{n+1,k} \left[c_{pv} \left(T^{n+1,k+1} - T_{ref} \right) + L_v \right] \nabla p_c^{n+1,k} \\
& \left. - K_{vT}^{n+1,k} \left[c_{pv} \left(T^{n+1,k+1} - T_{ref} \right) + L_v \right] \nabla T^{n+1,k+1} \right) \\
& - \frac{C_{TT}^{n+1} T^{n+1} - C_{TT}^n T^n}{\Delta t}
\end{aligned} \tag{1.40}$$

The system of linear equations is solved by Krylov subspace iteration solver, i.e. preconditioned conjugate gradient (PCG) with diagonal-based incomplete Cholesky (DIG) preconditioning. The convergence criteria for the Picard iteration is user-defined:

$$|p_c^{n+1,k+1} - p_c^{n+1,k}| \leq \delta p_c \tag{1.41}$$

$$|T^{n+1,k+1} - T^{n+1,k}| \leq \delta T \tag{1.42}$$

where $\delta p_c = \delta T = 10^{-2}$.

1.3 SOIL-PLANT-ATMOSPHERE CONTINUUM MODEL

In the present study, the components of the water potential inside the plants are not directly determined. The soil-plant-atmosphere continuum (SPAC) model that is integrated into the vegetation model is described in this section, implemented according the state-of-art techniques: (Idso 1977; Farquhar et al. 1980; Manzoni et al. 2011; Volpe et al. 2013; Manoli et al. 2014; Launiainen et al. 2015). The root-system of the plants are represented as a network-like structure assuming cooperative strategy among the individual roots and a bulk plant transpiration through a single xylem. We assume no water storage inside the plant and therefore, the water flux from soil to root $G_{v,root}$, from root to leaf through xylem $G_{v,xylem}$, and from leaf to air $G_{v,leaf}$ is in equilibrium, as depicted in Fig. 1.2:

$$G_{v,root} = G_{v,xylem} = G_{v,leaf} \tag{1.43}$$

and so, the atmospheric evaporative demand (AED) is dependent on the water availability near the roots of the plants.

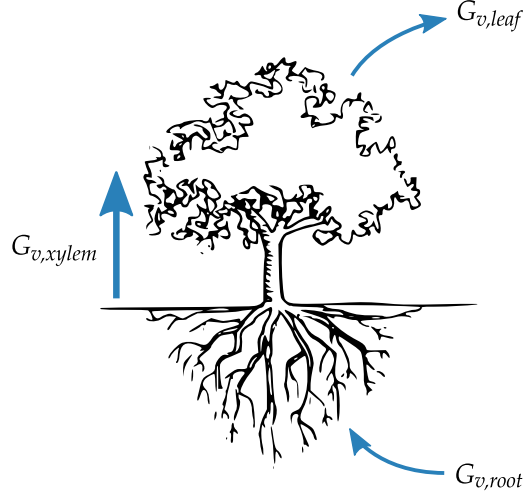


Figure 1.2: Soil-Plant-Atmosphere Continuum: The water balance between plant transpiration and root water uptake, $G_{v,root} = G_{v,xylem} = G_{v,leaf}$.

1.3.1 Water transport in soil-root system

The sink term s_r ($\text{kg m}^{-3} \text{s}^{-1}$) due to root water uptake in soil moisture transport equation (Eq. (1.24)) is simply defined as:

$$s_r = r g_{v,root} \quad (1.44)$$

where r ($\text{m}^2 \text{m}^{-3}$) is the root area density and $g_{v,root}$ ($\text{kg m}^{-2} \text{s}^{-1}$) is the root water uptake, i.e., the flux of water from root to soil. It is defined as:

$$g_{v,root} = k_{sr}^* (\psi_s - \psi_R) \quad (1.45)$$

where k_{sr}^* (s m^{-1}) is effective conductance of the soil-root system (i.e., rhizosphere), ψ_s (Pa) is the soil water potential, and ψ_R (Pa) is the (bulk) root water potential. The effective conductance of the soil-root system (or rhizosphere) k_{sr}^* (s m^{-1}) is given as:

$$k_{sr}^* = \frac{1}{|g|} \frac{k_s k_r}{k_s + k_r} \quad (1.46)$$

where g (m s^{-2}) is the gravitational acceleration, k_s (s^{-1}) is the soil conductance in the root region, and k_r (s^{-1}) is the conductance of the root system. The soil conductance in the root region k_s (s^{-1}) is defined as:

$$k_s = \alpha K r \quad (1.47)$$

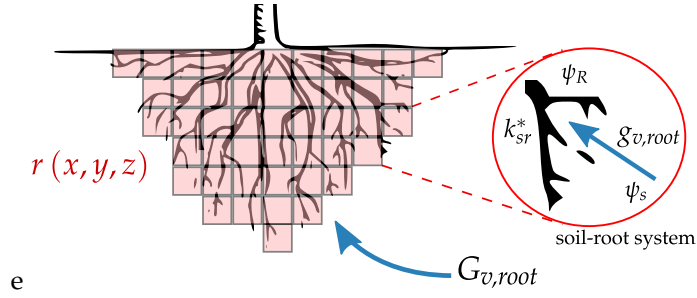


Figure 1.3: Soil-Plant-Atmosphere Continuum: The water transport in soil-root system.

where

$$\alpha = \sqrt{\left(\frac{L}{RAI}\right) \frac{1}{d}} \quad (1.48)$$

d (m) is the root diameter, L (m) is the root-depth height, and $RAI = \int r \, dz$ is the root area index ($\text{m}^2 \text{m}^{-2}$). The hydraulic conductivity in soil K (m s^{-1}) is given as:

$$K = K_{lp} |g| \quad (1.49)$$

where K_{lp} (s) being the liquid permeability defined in the Section 1.2.3. Finally, the conductance of the root system k_r (s^{-1}) is given as:

$$k_r = r \frac{\Delta z}{\beta} \quad (1.50)$$

where Δz is the vertical height of the root layer mesh and $\beta = 3 \times 10^8$ s.

Thus, the net root water uptake from the soil domain $G_{v,root}$ (kg s^{-1}) is given as:

$$G_{v,root} = \int_{\Omega_s} s_r \, dV = \int_{\Omega_s} r g_{v,root} \, dV \quad (1.51)$$

where Ω_s denotes the soil domain.

1.3.2 Water transport in xylem

The water flux through the plant in xylem $g_{v,xylem}$ ($\text{kg m}^{-2} \text{s}^{-1}$) is defined as:

$$g_{v,xylem}(\psi_L) = k_x^* (\psi_R - \psi_L) \quad (1.52)$$



Figure 1.4: Soil-Plant-Atmosphere Continuum: The water transport in plant xylem.

where k_x^* (s m^{-1}) is the effective xylem conductance, ψ_R (Pa) is the (bulk) root water potential, and ψ_L (Pa) is the (bulk) leaf water potential. The net water flux $G_{v,xylem}$ (kg s^{-1}) is given as:

$$G_{v,xylem} = \int_{\partial\Omega_x|_s} g_{v,xylem} \, dA = g_{v,xylem} A_x \quad (1.53)$$

where A_x (m^2) is the xylem cross-sectional area. The effective xylem conductance k_x^* (s m^{-1}) of water is:

$$k_x^* = k_x \rho_l \quad (1.54)$$

where plant xylem conductance k_x ($\text{m Pa}^{-1} \text{s}^{-1}$) is modeled using a “*vulnerability curve*” approach. The xylem conductance becomes exponentially smaller with increasing leaf water potential (Volpe et al. 2013). This empirical model is based on plant response to the vulnerability to xylem cavitation and embolism that could occur at high water potential gradients. The xylem conductance k_x ($\text{m Pa}^{-1} \text{s}^{-1}$) is defined by:

$$k_x = k_{x,max} \exp \left\{ - \left(- \frac{\psi_L}{d} \right)^c \right\} \quad (1.55)$$

where $k_{x,max}$ ($\text{m Pa}^{-1} \text{s}^{-1}$) is the maximum xylem conductance, and c and d are fit-coefficients (Volpe et al. 2013).

1.3.3 Water transport from leaf to air

The leaf transpiration rate $g_{v,leaf}$ ($\text{kg m}^{-2} \text{s}^{-1}$) is defined in ??, and is simply defined as:

$$g_{v,leaf} = k_{st,v}^* \left(\frac{p_{v,leaf} - p_v}{p} \right) \quad (1.56)$$

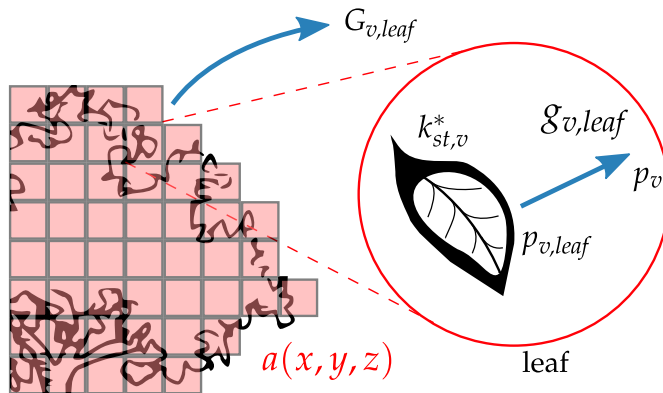


Figure 1.5: Soil-Plant-Atmosphere Continuum: The water transport from leaf to air.

where $p_{v,leaf}$ (Pa) is the vapor pressure at the leaf, p_v (Pa) is the ambient vapor pressure, p (Pa) is ambient pressure, and $k_{st,v}^*$ ($\text{kg m}^{-2} \text{s}^{-1}$) is the effective stomatal conductance to water vapor. It is defined as:

$$k_{st,v}^* = M_v k_{st,v} \quad (1.57)$$

where $M_v = 1.8015 \times 10^{-2} \text{ kg mol}^{-1}$ is the molar mass of water vapor and $k_{st,v}$ ($\text{mol m}^{-2} \text{s}^{-1}$) is the stomatal conductance to water vapor in molar units (the molar unit is commonly used in plant-science community). The stomatal conductance to water vapor is described in detail in Section 1.3.4.

The net plant transpiration rate $G_{v,leaf}$ (kg s^{-1}) is given as:

$$G_{v,leaf} = \int_{\Omega_a} a g_{v,leaf} dV \quad (1.58)$$

where a ($\text{m}^2 \text{m}^{-3}$) is the leaf area density and Ω_a denotes the air domain. As the water mass flux to the atmosphere is in equilibrium with the water vapor flux through xylem, i.e., as shown in Eq. (1.43), we can equate Eq. (1.58) to Eq. (1.53):

$$G_{v,leaf} = G_{v,xylem} \quad (1.59)$$

and so:

$$G_{v,leaf} = k_x^* (\psi_R - \psi_L) A_x \quad (1.60)$$

Therefore, we can determine the root water potential ψ_R as follows:

$$\psi_R = \psi_L + \frac{G_{v,leaf}}{A_x k_x^*} \quad (1.61)$$

and is simply dependent on the leaf water potential ψ_L (Pa), the net plant transpiration rate $G_{v,leaf}$ (kg s^{-1}), effective xylem conductance k_x^* (s m^{-1}), and the xylem cross-

sectional area A_x (m^2). Additionally, we can also take in account of the influence of graviational potential change due to height of the plant as follows:

$$\psi_R = \psi_L + \frac{G_{v,leaf}}{A_x k_x^*} + \underbrace{\rho_l g H}_{\psi_g} \quad (1.62)$$

For a plant with a plant canopy height of $H = 10$ m, the additional potential is $\psi_g = 0.1$ MPa and typically is negligible compared to the contribution of leaf water potential.

1.3.4 Stomatal model with water stress sensitivity

The photosynthetic reaction creates carbohydrate and oxygen from light, water, and CO_2 . Therefore, the photosynthetic rate f_c ($\text{mol m}^{-2} \text{s}^{-1}$) defined as the rate of CO_2 assimilated by the plant (i.e., denoted also as A_n (in plant-science) or $G_{c,leaf}$ (in building physics), also known as assimilation rate) is directly related to atmospheric condition such as CO_2 concentration, availability of light and temperature. The assimilation rate is defined through Fickian diffusion law as: The Fickian diffusion through stomata is given as:

$$f_c = k_{st} (c_a - c_i) \quad (1.63)$$

where k_{st} ($\text{mol m}^{-2} \text{s}^{-1}$) is the (molar) stomatal conductance to CO_2 (note that for now we neglect the boundary layer conductance), c_i (mol mol^{-1}) is the intercellular CO_2 concentration, and c_a (mol mol^{-1}) is the ambient CO_2 concentration. However, during the opening of the stomata, additional moisture is lost by evaporation due to exposure of stomatal cavity to the atmosphere. Therefore, the transpiration rate f_v ($\text{mol m}^{-2} \text{s}^{-1}$) (i.e. denoted also as f_e (in plant-science) or $G_{v,leaf}$ (in building physics), and also known as water use) is dependent on the atmospheric humidity and the availability of water for transpiration (Ball1987; Leuning et al. 1995). It is similarly described, based on Fickian diffusion process:

$$f_v = k_{st,v} \left(\frac{p_{v,i} - p_v}{p} \right) \quad (1.64)$$

where $k_{st,v}$ ($\text{mol m}^{-2} \text{s}^{-1}$) is the (molar) stomatal conductance to water vapor, $p_{v,i}$ (Pa) is the intercellular vapor pressure, and p_v (Pa) is the ambient vapor pressure. The water vapor stomatal conductance is related to the CO_2 stomatal conductance as:

$$k_{st,v} = a_c k_{st} \quad (1.65)$$

where $a_c = 1.6$ is the relative diffusion of water vapor to CO_2 . Furthermore, $p_{v,i} = p_{v,sat}(T_l)$ (Pa) where the intercellular vapor pressure inside the stomatal cavity is assumed to be at saturation at the leaf temperature T_l .

So, the stomatal regulatory function is can be modeled through appropriate stomatal conductance. A generally accepted theory of plant response is that the plant regulates the stomatal aperture to optimize the photosynthetic rate for a given transpiration rate. Thus, the function of vegetation can be simplified as just maximizing the pho-

tosynthesis (or CO₂ assimilation) for a given transpiration rate (water use) (Medlyn et al. 2011) and the water use efficiency (WUE) quantifies the efficiency of the plant of reaching this target:

$$WUE = \frac{f_c}{f_v} \quad (1.66)$$

The “*stomatal optimality model*” reflects the theory of such stomatal behavior (Cowan 1978). The optimal stomatal control is derived from the minimization problem described by the Lagrangian:

$$\mathcal{L}(k_{st}) = f_c - \lambda f_v \quad (1.67)$$

where λ (mol mol⁻¹) is a Lagrange multiplier and represents the marginal water cost of plant carbon gain (Katul et al. 2010; Medlyn et al. 2011; Manoli et al. 2014) and $f_c = f_c(k_{st})$ and $f_v = f_v(k_{st})$ are a function of stomatal conductance. Cowan (1978) shows that optimal stomatal behaviour is at the minima of the Lagrangian:

$$\frac{\partial \mathcal{L}}{\partial k_{st}} = 0 \quad (1.68)$$

leading to the following constraint:

$$\lambda = \frac{\partial f_v}{\partial k_{st}} \frac{\partial k_{st}}{\partial f_c} \quad (1.69)$$

or simply:

$$\lambda = \frac{\partial f_v}{\partial f_c} \quad (1.70)$$

Following these constraints, the stomatal conductance k_{st} can be determined, given that unknowns in the assimilation rate f_c are closed. To provide a closure for the assimilation rate, the assimilation rate f_c described from the perspective of photochemical reaction model is also used. The Farquhar model of photosynthesis describing the biochemical demand function is given as:

$$f_c = \frac{a_1 c_i}{a_2 + s c_a} \quad (1.71)$$

where c_i (mol mol⁻¹) is the intercellular CO₂ concentration, c_a (mol mol⁻¹) is the ambient CO₂ concentration, and a_1 and a_2 are parameters dependent on whether photosynthetic reaction rate is limited by light or RuBisCO (Rubilose biphosphate (RuBP) carboxylase-oxygenase) (Farquhar et al. 1980; Katul et al. 2010), and $s = 0.7$ is the constant representing long-term intercellular to ambient CO₂ concentration ratio (Volpe et al. 2013). A detailed description of calculating a_1 and a_2 are given in Section 1.3.5.

To solve for the stomatal conductance k_{st} , the remaining unknown is the intercellular CO₂ concentration c_i . We can determine this by equating Fickian CO₂ flux (Eq. (1.63)) to the Farquhar biochemical demand (Eq. (1.71)):

$$f_c = \frac{a_1 c_i}{a_2 + s c_a} = k_{st} (c_a - c_i) \quad (1.72)$$

and rewriting it for c_i , we get:

$$c_i = c_a \frac{a_2 + s c_a}{a_1 / k_{st} + a_2 + s c_a} \quad (1.73)$$

So, substituting Eq. (1.73) back into the biochemical demand function (Eq. (1.71)), the assimilation rate becomes a closed-problem:

$$f_c = \frac{k_{st} a_1 c_a}{a_1 + k_{st} (a_2 + s c_a)} \quad (1.74)$$

where only the k_{st} is the remaining unknown. Finally, the stomatal conductance k_{st} can be determined by solving Eq. (1.68):

$$\frac{\partial \mathcal{L}}{\partial k_{st}} = \frac{\partial f_c}{\partial k_{st}} - \lambda \frac{\partial f_v}{\partial k_{st}} = 0 \quad (1.75)$$

Substituting Eq. (1.74) and Eq. (1.64) into Eq. (1.75), we have:

$$\frac{\partial}{\partial k_{st}} \left[\left(\frac{k_{st} a_1 c_a}{a_1 + k_{st} (a_2 + s c_a)} \right) - \lambda a_c k_{st} VPD \right] = 0 \quad (1.76)$$

where $VPD \equiv (p_{v,i} - p_v) / p$ (mol mol⁻¹). Solving Eq. (1.76), we get:

$$\frac{a_1^2 c_a}{[a_1 + k_{st} (a_2 + s c_a)]^2} - \lambda a_c VPD = 0 \quad (1.77)$$

and rewriting it for k_{st} , we obtain:

$$k_{st} = \frac{a_1}{a_2 + s c_a} \left(-1 + \sqrt{\frac{c_a}{a_c \lambda VPD}} \right) \quad (1.78)$$

Additionally, in literature it is known that stomata does not completely close during night allowing for respiration. Therefore, taking this into account:

$$k_{st} = \frac{a_1}{a_2 + s c_a} \left(-1 + \sqrt{\frac{c_a}{a_c \lambda VPD}} \right) + k_{st,n} \quad (1.79)$$

where $k_{st,n}$ (mol m⁻² s⁻¹) is the nocturnal stomatal conductance ($k_{st,n} = 0.018$ mol m⁻² s⁻¹, (Manoli et al. 2014)). Thus, we obtain a stomatal model that is a function of the CO₂ assimilation (through parameters a_1 , a_2 and c_a), atmospheric evaporative demand

(AED) (through parameter VPD), and the Lagrangian multiplier λ which represents the marginal water cost of plant carbon gain. Therefore, λ reflects the sensitivity to water availability is also commonly known as the *marginal water use efficiency*. It is empirically related to the leaf water potential $\lambda = \lambda(\psi_L)$ (Katul et al. 2010; Manoli et al. 2014) and so, the stomatal response change to water availability is reflected through the change in leaf water potential ψ_L . The marginal WUE is determined from experimental measurements of plant photosynthesis, transpiration and stomatal conductance, and solving for the gradient of Eq. (1.66). An empirical model of marginal WUE, λ , as a function of leaf water potential ψ_L (Katul et al. 2010; Manoli et al. 2014), is given as:

$$\lambda(\psi_L) = \lambda_{max}^* \frac{c_a}{c_a^*} \exp \left\{ -\beta \left(\langle \psi_L \rangle_{24h} - \psi_{L,max} \right)^2 \right\} \quad (1.80)$$

where ψ_L is assumed to vary slowly such that $\langle \psi_L \rangle_{24h}$ is fixed within the secant iteration, λ_{max}^* is the marginal WUE under well-watered soil condition at reference CO_2 concentration $c_a^* = 400 \mu\text{mol mol}^{-1}$ or parts-per-million (ppm), β is the plant-specific sensitivity parameter (Huang et al. 2017).

Now that, we have closed k_{st} through Eq. (1.78), the intercellular CO_2 equation can be further simplified. Substituting Eq. (1.78) into Eq. (1.73), it becomes:

$$c_i = \left(c_a - \sqrt{a_c \lambda VPD c_a} \right) \quad (1.81)$$

meaning that it is only dependent on the ambient CO_2 concentration, vapor pressure deficit, and the marginal water use efficiency. Substituting Eq. (1.81) into Eq. (1.74), gives:

$$f_c = \frac{a_1 c_a}{a_2 + s c_a} \left(1 - \sqrt{a_c \lambda VPD c_a} \right) \quad (1.82)$$

1.3.5 Assimilation rate

As the photosynthesis can either be *light-limited* or *Rubisco-limited*, the true assimilation rate f_c is given as:

$$f_c = \min \left(f_c^l, f_c^r \right) \quad (1.83)$$

where f_c^l is the assimilated limited by light and f_c^r is assimilation rate limited by RuBisCO. Note that it is also possible to incorporate the dark (or night) respiration and in that case $f_c = \min \left(f_c^l, f_c^r \right) - r_d$, but is not modeled in our study.

Light-limited

If assimilation is *light-limited*, a_1 and a_2 is defined as (Katul et al. 2010; Manoli et al. 2014):

$$a_1 = \underbrace{\alpha_p e_m}_{\gamma} Q_p \quad (1.84)$$

and

$$a_2 = 2c_p \quad (1.85)$$

where α_p is the leaf absorptivity of photosynthetically active radiation (PAR), e_m is the maximum quantum efficiency of the leaf, $\gamma = 0.015$ is the apparent quantum yield, Q_p ($\text{mol m}^{-2} \text{s}^{-1}$) is the flux of incoming PAR, and c_p (mol mol^{-1}) is the the CO_2 compensation point. The CO_2 compensation point is determined as:

$$c_p = \frac{K_c}{2K_o} C_{o,a} \frac{k_o}{k_c} \quad (1.86)$$

where $k_c = 2.5 \text{ s}^{-1}$ and $k_o = 0.18k_c$, and:

$$K_c = K_{c,25} \exp \{ \gamma_c (T_l - 298.15) \} \quad (1.87)$$

$$K_o = K_{o,25} \exp \{ \gamma_o (T_l - 298.15) \} \quad (1.88)$$

are Michaelis constant for CO_2 and O_2 inhibition (referenced at 25°C), and $C_{o,a} = 0.21 \text{ mol mol}^{-1}$ is the oxygen concentration in the atmosphere (Farquhar et al. 1980), with $K_{c,25} = 3 \times 10^{-3} \text{ mol mol}^{-1}$, and $K_{o,25} = 0.3 \text{ mol mol}^{-1}$. Thus, substituting Eq. (1.86) into Eq. (1.85), and Eqs. (1.84) and (1.85) into Eq. (1.74), we get the light-limited assimilation rate f_c^l as:

$$f_c^l = \frac{\gamma Q_p c_i}{2c_p + s c_a} \quad (1.89)$$

Rubisco-limited

If the assimilation rate is *Rubisco-limited*, a_1 and a_2 is defined as (Katul et al. 2010; Manoli et al. 2014):

$$a_1 = V_{cmax} \quad (1.90)$$

and

$$a_2 = K_c \left(1 + \frac{C_{o,a}}{K_o} \right) \quad (1.91)$$

where $V_{c,max}$ is the maximum carboxylation capacity (referenced at 25°C). The maximum carboxylation capacity is given as:

$$V_{cmax} = V_{cmax,25} \frac{\exp \{ 0.088 (T_l - 298.15) \}}{1 + \exp \{ 0.29 (T_l - 314.15) \}} \quad (1.92)$$

where T_l (K) is the leaf temperature, $V_{cmax,25} = 5.9 \times 10^{-5} \text{ mol m}^{-2} \text{s}^{-1}$, $\gamma_c = 0.074$, and $\gamma_o = 0.015$. Thus, substituting Eqs. (1.90) and (1.91) into Eq. (1.74), the Rubisco-limited assimilation rate is given as:

$$f_c^r = \frac{V_{cmax} c_i}{K_c \left(1 + \frac{C_{o,a}}{K_o} \right) + s c_a} \quad (1.93)$$

1.3.6 Numerical strategy for solving leaf water potential

The water transport through the plant from soil to root, from root to xylem, through the xylem, and finally, from leaf stomata to air is a closed-problem once the leaf water potential is known. The leaf water potential is determined from Eq. (1.43):

$$G_{v,leaf}(\psi_L) = G_{v,root}(\psi_L) \quad (1.94)$$

As an optimization problem, it is defined as:

$$\arg \min_{\psi_L} \mathcal{G}(\psi_L) = \left| G_{v,leaf} - G_{v,root} \right| \quad (1.95)$$

As this is a non-linear closure problem (Manoli et al. 2014), a secant method is employed to iteratively converge to the leaf water potential. The $j + 1^{\text{th}}$ leaf water potential estimate is determined as:

$$\psi_L^{j+1} = \psi_L^j - G(\psi_L^j) \frac{\psi_L^j - \psi_L^{j-1}}{G(\psi_L^j) - G(\psi_L^{j-1})} \quad (1.96)$$

where the initial estimate of $\psi_L^{j=0} = 0$ MPa and $\psi_L^{j=1} = -10$ MPa and with the additional constraint that $-10 \leq \psi_L \leq 0$ MPa, enforcing that leaf water potential is negative and not larger than -10 MPa. The detailed solution strategy for determining for coupling all the models is detailed in next section.

1.4 COUPLED AIR-SOIL-VEGETATION-RADIATION MODEL

The numerical model for air domain, solid domains (soil, ground, building), the radiation model and the vegetation model is implemented into OpenFOAM. The solid and air domains are coupled at regular intervals t^m defined as exchange timesteps or air time steps (Saneinejad et al. 2014; Kubilay et al. 2018). The fluxes between air and solid domain consisting for thermal, moisture and radiative transfers are coupled at this step, chosen to be 10 min. At each t^m , the air domain is assumed to the quasi-steady and solving using steady-state RANS approach converged when residuals of ρ , u , h , k , ε are below threshold. During the steady-state computation, the leaf energy balance is evaluated periodically to correct the heat and mass fluxes, $q_{sen,leaf}$ and $g_{v,leaf}$, respectively.

1.5 COUPLING ALGORITHM

The numerical model for air domain, solid domains (soil, ground, building), the radiation model and the vegetation model is implemented into OpenFOAM. The solid and air domains are coupled at regular intervals t^m defined as exchange timesteps or air time steps (Saneinejad et al. 2014; Kubilay et al. 2018). The fluxes between air and solid

domain consisting for thermal, moisture and radiative transfers are coupled at this step, chosen to be 10 min. At each t^m , the air domain is assumed to the quasi-steady and solving using steady-state RANS approach converged when residuals of ρ , u , h , k , ε are below threshold.

1.5.1 Air domain

The air domain is solved using m pseudo steady-state timesteps. The diurnal cycle is split into pseudo steady-state timesteps of $\Delta t^m = 10$ min (i.e., 8640 time steps in a 24 hrs). At each steady-state timestep t^m , the quasi steady-state RANS model is solved for the fluid equations: ρ , u , h , k , and ε . During the steady-state computation, the *leaf energy balance* (LEB) model is solved to determine the heat and mass fluxes, $q_{sen,leaf}$ and $g_{v,leaf}$, respectively. The algorithm for solving the air domain from $t^m \rightarrow t^{m+1}$ is as follows:

1. Update the radiation fields in the air domain using q_{rad} from building surfaces and determined $q_{r,tw}$ and $q_{r,sw}$.
2. Solve *leaf energy balance* (LEB) model:
 - a) Calculate radiative flux $q_{rad,leaf}$ using ??.
 - b) Calculate the stomatal and aerodynamic resistances r_s and r_a using ?? and ??, respectively.
 - c) Perform an initial estimate of leaf temperature $T_{leaf} = T$.
 - d) Calculate saturated vapor pressure at the leaf surface $p_{vsat,leaf} = f(T_{leaf})$.
 - e) Calculate latent heat flux $q_{lat,leaf}$ using ??.
 - f) Correct leaf temperature T_{leaf} using ??.
 - g) Repeat steps (d) to (f) until the leaf temperature has converged ($\epsilon < 10^{-8}$).
3. Calculate all vegetation source terms s_ρ , s_u , s_T , s_w , s_k and s_ε using ???????????.
4. Solve for the steady-state air flow field for t^{m+1} , ??-??.
5. Repeat steps (2) to (4) until residuals of ??-?? have reached the convergence limit of $\epsilon < 10^{-6}$.

1.5.2 Solid domain

The solid domain describes the heat and mass transport in urban structures such as building facade, pavement, road and the ground (i.e., soil). Each of these “sub” domains consists of n adaptive solid timesteps with $\Delta t^n < \Delta t^m$ (Janssen 2002; Kubilay et al. 2018). At the beginning of the solid domain iteration, the thermal, moisture and radiative transfers are updated providing the necessary boundary conditions for wall

boundaries. For each of n solid timesteps, the linearized heat and mass transport equation are solved using k Picard iterations. In only the soil sub-domain, for each of these k Picard iteration, the root water uptake is determined through j secant iterations. The algorithm of solving such soil sub-domain is given as:

1. k Picard iterations solving for the linearized heat and mass transport transport equations:
 - (a) Calculate marginal WUE $\lambda (\langle \psi_L \rangle_{24h})$.
 - (b) Calculate stomatal conductance k_{st} , constant in the secant iteration.
 - (c) Calculate assimilation rate f_c and transpiration rate f_v .
 - (d) Calculate net transpiration rate $G_{v,leaf}$.
 - (e) Calculate effective soil-root conductance k_{sr}^* .
 - (f) j Secant iterations solve for leaf water potential ψ_L .
 - (a) Initial guess of leaf water potential, $\psi_L^{j=0} = 0$ MPa, $\psi_L^{j=1} = -10$ MPa.
 - (b) Calculate effective xylem conductance k_x^* .
 - (c) Calculate root water potential ψ_R^j .
 - (d) Calculate root uptake $g_{v,root}$ and net root uptake $G_{v,root}$.
 - (e) Calculate cost function \mathcal{G} .
 - (f) Correct leaf water potential using secant method $\psi_L^j \rightarrow \psi_L^{j+1}$.
 - (g) Repeat till leaf water potential is converged, $\delta\psi_L \leq \epsilon$.
 - (g) Calculate the sink in soil moisture due to root water uptake s_r .
 - (h) Solve linearized form of heat and mass equation using PCG until $\delta p_c = \delta T = 10^{-2}$, repeating steps before.
2. Use the final surface temperature T_s^N to update the radiation model updating $q_{r,lw}$ fluxes from all surfaces.
3. Final surface temperature T_s^N and moisture fluxes g_v^N are boundary condition for the air domain for $t^m \rightarrow t^{m+1}$.

BIBLIOGRAPHY

- Idso, S. B. (1977). *An Introduction to Environmental Biophysics*. Vol. 6. 4, p. 474.
- Cowan, I. (1978). "Stomatal Behaviour and Environment." In: *Adv. Bot. Res.* Vol. 37, pp. 117–228.
- Farquhar, G. D., S. Von Caemmerer, and J. A. Berry (1980). "A Biochemical Model of Photosynthetic CO₂ Assimilation in Leaves of C₃ Species." In: *Planta* 149, pp. 78–90.
- Leuning, R., F. M. Kelliher, D. G. G. de Pury, and E. D. Schulze (1995). "Leaf nitrogen, photosynthesis, conductance and transpiration: Scaling from leaves to canopies." In: *Plant, Cell Environ.* 18.10, pp. 1183–1200.
- Janssen, H. (2002). *The influence of soil moisture transfer on building heat loss via the ground*. Vol. 39. 7, pp. 825–836.
- Carmeliet, J. (2005). *Coupled heat and mass transfer: Theory, Moisture transport properties*. Tech. rep.
- Nobel, P. S. (2009). *Physicochemical and Environmental Plant Physiology*. Elsevier Science.
- Katul, G., S. Manzoni, S. Palmroth, and R. Oren (Mar. 2010). "A stomatal optimization theory to describe the effects of atmospheric CO₂ on leaf photosynthesis and transpiration." In: *Ann. Bot.* 105.3, pp. 431–442.
- Defraeye, T. (2011). "Convective heat and mass transfer at exterior building surfaces." Phd Thesis. Katholieke Universiteit Leuven.
- Manzoni, S., G. Vico, G. Katul, P. A. Fay, W. Polley, S. Palmroth, and A. Porporato (2011). "Optimizing stomatal conductance for maximum carbon gain under water stress: A meta-analysis across plant functional types and climates." In: *Funct. Ecol.* 25.3, pp. 456–467.
- Medlyn, B. E., R. A. Duursma, D. Eamus, D. S. Ellsworth, I. C. Prentice, C. V. Barton, K. Y. Crous, P. De Angelis, M. Freeman, and L. Wingate (2011). "Reconciling the optimal and empirical approaches to modelling stomatal conductance." In: *Glob. Chang. Biol.* 17.6, pp. 2134–2144.
- Liu, X. (2012). "suGWFOam : An Open Source Saturated-Unsaturated GroundWater Flow Solver based on OpenFOAM." In: *Report* 01, pp. 1–54.
- Saneinejad, S. (2013). "The influence of evaporative cooling on the micro-climate and thermal comfort in a street canyon." PhD thesis, p. 201.
- Volpe, V., M. Marani, J. D. Albertson, and G. Katul (2013). "Root controls on water redistribution and carbon uptake in the soil-plant system under current and future climate." In: *Adv. Water Resour.* 60, pp. 110–120.
- Kubilay, A. (2014). "Numerical simulations and field experiments of wetting of building facades due to wind-driven rain in urban areas." PhD thesis, p. 319.
- Manoli, G., S. Bonetti, J. C. Domec, M. Putti, G. Katul, and M. Marani (2014). "Tree root systems competing for soil moisture in a 3D soil-plant model." In: *Adv. Water Resour.* 66, pp. 32–42.

- Saneinejad, S., P. Moonen, and J. Carmeliet (2014). "Coupled CFD, radiation and porous media model for evaluating the micro-climate in an urban environment." In: *J. Wind Eng. Ind. Aerodyn.* 128, pp. 1–11.
- Launiainen, S., G. G. Katul, A. Lauren, and P. Kolari (2015). "Coupling boreal forest CO₂, H₂O and energy flows by a vertically structured forest canopy – Soil model with separate bryophyte layer." In: *Ecol. Modell.* 312, pp. 385–405.
- Huang, C.-W., J.-C. Domec, E. J. Ward, T. Duman, G. Manoli, A. J. Parolari, and G. G. Katul (2017). "The effect of plant water storage on water fluxes within the coupled soil-plant system." In: *New Phytol.* 213.3, pp. 1093–1106.
- Kubilay, A., D. Derome, and J. Carmeliet (June 2018). "Coupling of physical phenomena in urban microclimate: A model integrating air flow, wind-driven rain, radiation and transport in building materials." In: *Urban Clim.* 24, pp. 398–418.

COLOPHON

This document was typeset in L^AT_EX using the typographical look-and-feel classicthesis.
The bibliography is typeset using bibl_{at}ex with natbib.